The Journal of Experimental Biology 205, 1209–1219 (2002)
Printed in Great Britain © The Company of Biologists Limited 2002
JEB3943

Characterization of yeast V-ATPase mutants lacking Vph1p or Stv1p and the effect on endocytosis

Natalie Perzov, Vered Padler-Karavani, Hannah Nelson* and Nathan Nelson
Department of Biochemistry, The George S. Wise Faculty of Life Sciences, Tel Aviv University, Tel Aviv 69978, Israel

*Author for correspondence (e-mail: nelson@post.tau.ac.il)

Accepted 11 February 2002

Summary

Subunit a of V-ATPase in the yeast *Saccharomyces cerevisiae*, in contrast to its other subunits, is encoded by two genes *VPH1* and *STV1*. While disruption of any other gene encoding the V-ATPase subunits results in growth arrest at pH 7.5, null mutants of Vph1p or Stv1p can grow at this pH. We used a polyclonal antibody to yeast Stv1p and a commercially available monoclonal antibody to Vph1p for analysis of yeast membranes by sucrose gradient fractionation, and two different vital dyes to characterize the phenotype of *vph1Δ* and *stv1Δ* mutants as compared to the double mutant and the wild-type cells. Immunological assays of sucrose gradient fractions revealed that the amount of Stv1p was elevated in the *vph1Δ* strain, and that vacuoles purified by this method with no detectable endosomal contamination contain an assembled V-ATPase complex, but with much lower activity than the wild type. These results suggest that Stv1p compensates for the loss of Vph1p in the *vph1Δ* strain. LysoSensor Green DND-189 was used as a pH sensor to demonstrate unexpected changes in vacuolar acidification in *stv1Δ* as the Vph1p-containing V-ATPase complex is commonly considered to acidify the vacuoles. In the *vph1Δ* strain, the dye revealed slight but definite acidification of the vacuole as well. The lipophilic dye FM4-64 was used as an endocytic marker. We show that the null V-ATPase mutants, as well as the *vph1Δ* one, markedly slow down endocytosis of the dye.

Key words: V-ATPase, subunit a, yeast, *Saccharomyces cerevisiae*, biogenesis, endocytosis, proton pumping.

Introduction

Vacuolar ATPases are multisubunit complexes, found in all eukaryotic cells, which are responsible for the acidification of intracellular compartments. These compartments include endosomes, lysosomes, Golgi membranes, clathrin-coated vesicles, several types of secretory granules and the central vacuoles of plants and yeast (Nelson and Harvey, 1999). Each of these intracellular compartments requires a specific internal pH that is generated by the V-ATPase function (Grabe and Oster, 2001). In a single cell, V-ATPases can be involved in a variety of essential cellular functions, including receptor-mediated endocytosis, post-translational modification, protein sorting along the secretory pathway, protein degradation and secondary transport (Stevens and Forgac, 1997). V-ATPase energizes the vacuolar system by driving the translocation of protons across the vacuolar membrane into the lumen at the expense of ATP hydrolysis.

In common with the evolutionarily related F-ATPase, whose primary function in eukaryotic cells is to form ATP, V-ATPase is composed of two functional domains. The peripheral V_1 domain, which is responsible for ATP hydrolysis, contains at least eight subunits, denoted as subunits A through H (Stevens and Forgac, 1997; Nelson and Harvey, 1999). The membrane V_o domain consists of at least five subunits (*a*, *c*, *c′*, *c″* and *d*) and functions in proton translocation (Powell et al., 2000; Stevens and Forgac, 1997). In most of the eukaryotic organisms studied, a null mutation in the V-ATPase gene results in a lethal phenotype. In contrast, yeast cells lacking V-ATPase activity due to the same null mutation can survive, but only in a buffered medium at pH 5.5 (Nelson and Nelson, 1990). These mutations exhibit a conditionally lethal phenotype in which cells cannot grow at a pH higher than 7.0 or various other medium conditions (Nelson and Nelson, 1990). This feature makes yeast one of the favorite organisms for V-ATPase studies. Furthermore, the yeast genome has one gene encoding each subunit of the V-ATPase, except for *VPH1* and *STV1*, which encode two isoforms of the 100 kDa a subunit (Vph1p and Stv1p). Disruption of both subunits is necessary to produce the null V-ATPase mutant phenotype (Manolson et al., 1992, 1994), which creates a unique opportunity to study the role of isoforms in the V-ATPase subunits. In other organisms, many of the V-ATPase subunit isoforms were demonstrated to be tissue-specific (Futai et al., 2000), yet some were found in specific locations in the same cells (Toyomura et al., 2000). In yeast, Vph1p was assigned to the vacuole, and a Golgi and/or endosome localization was proposed for Stv1p (Manolson et al., 1994). These observations suggest that

subunit a may be responsible for the V-ATPase localization in specific subcellular compartments and/or regulation of enzymatic activity, which implies that there should be specific and distinct phenotypes for both mutants. The *vph1*Δ mutant is unable to accumulate Quinacrine in the vacuole, and therefore appears to be defective in vacuolar acidification, but no phenotype has been described for absence of Stv1p, and the *stv1*Δ mutant was reported to be identical to the wild type (Manolson et al., 1994).

Properties of V-ATPase complexes containing both disrupted Vph1 and Stv1 genes (double-deletion mutant) were recently studied with overexpression of each gene cloned into a yeast shuttle vector (Kawasaki-Nishi et al., 2001). It was demonstrated that a complex containing Stv1p showed lower assembly with the catalytic subunits and a lower ratio of proton transport to ATP hydrolysis than the V-ATPase complex containing Vph1p.

In this paper, we reinvestigate the subcellular locations of the Vph1p and Stv1p and also define the characteristics of the separate *vph1*Δ and *stv1*Δ phenotypes in comparison to the wild type and double-deletion mutant. We used a new pH-sensitive LysoSensor Green DND-189 dye to determine the extent of acidification within the intracellular compartments in both wild type and null mutants for each of the two isoforms of subunit a. The V-ATPase was suggested to be directly involved in endocytosis and membrane fusion (Wendland et al., 1998; Ungermann et al., 1999; D'Hondt et al., 2000; Peters et al., 2001). Using the endocytic marker FM 4-64 we show that the endocytic process is inhibited whenever there is a decrease in the cellular V-ATPase activity.

Materials and methods

Strains, media and reagents

The 'wild type' strain used is a haploid *S. cerevisiae* W303 (*MATa/α trp1 ade2 his3 leu2 ura3*). The other haploid strains used in this work are: *vma3Δ* (*MATa ade2 trp1 ura3 his3 VMA3::LEU2*); *stv1Δ* (*MATa ade2 ura3 his3 leu2 STV1::TRP1*); *vph1Δ/stv1Δ* (*MATa ade2 trp1 ura3 his3 VPH1::LEU2 STV1::URA3*); *vph1Δ* (*MATα ade2 ura3 his3 leu2 trp1 VPH1::LEU2*); *vma8Δ* (*MATα ade2 ura3 his3 leu2 trp1 VMA8::LEU2*); *vtc1Δ* (*MATa ade2 trp1 ura3 his3 leu2 VTC1::URA3*). The cells were grown in a YPD medium containing 1% yeast extract, 2% bactopeptone and 2% dextrose. The medium was buffered as previously described (Noumi et al., 1991).

Preparation of yeast strains

All the yeast strains used in this work were prepared as previously described (*vma3Δ*, Nelson and Nelson, 1990; *vma8Δ* and *vtc1Δ*, Cohen et al., 1999). Constructs for disruption of the *VPH1* and *STV1* genes were prepared as follows. Each gene was amplified from yeast genomic DNA by polymerase chain reaction (PCR) with specific primers, cloned into pGEM-T easy or pBluescript SK, respectively. For *VPH1*, a fragment of 610 base pairs (bp) was deleted by digestion with *Hinc*II and *Eco*RV, and a blunt-end *LEU2* marker was inserted in its place. For *STV1* (which was cloned into the *Kpn*I–*Bam*HI sites of pBluescript) a 2360 bp fragment was deleted by digestion with *Eco*Rl and *Xho*I, filled in and a blunt-end *TRYP1* or *URA3* marker inserted. The constructs were excised using appropriate enzymes at either end and used for yeast W303 or *vph1Δ* (haploid strains) transformation. Homologous recombination and null V-ATPase phenotypes were checked as previously described (Cohen et al., 1999).

Antibody preparation and western analysis

Polyclonal antibody against Stv1p was obtained by injecting rabbits with a chimeric protein containing the maltose-binding protein and hydrophilic sequence of amino acid residues 231–436 of Stv1p. The DNA fragment encoding these amino acids was amplified by PCR with introduced *Eco*RI and *Hin*dIII restriction sites. The amplified DNA fragment was cloned in-frame to the maltose-binding protein in the plasmid PMAL-C (New England Biolab). Following sequence verification, 500 ml of bacterial culture was grown to A_{600}=0.5, induced with isopropyl-β-D-thiogalactoside (IPTG) for 3 h and harvested by centrifugation at 4000 ***g***. The cells were broken using a French press and the protein purified on a column containing maltose–agarose. The fractions containing the chimeric protein were dissociated by SDS, loaded on a preparative gel and electrophoresed. The gel was briefly stained by Coomassie Blue, the identified protein band cut out and the fusion protein was electroeluted. About 0.25 mg fusion protein was injected into rabbits as previously described (Nelson, l983). Polyclonal antibody against Sec14p was prepared as a chimeric protein containing the maltose-binding protein and the whole open-reading frame sequence of the Sec14p was prepared using a procedure similar to that described for the Stv1p antibody. Monoclonal antibodies that recognize Vph1p (10D7-A7-B2), CPY (10A5-B5) and Pep12p (2C3G4) were from Molecular Probes, Inc. Polyclonal antibody against the purified Pma1p was raised in rabbits and used at a dilution of 1:10,000. Antibody against Sed5p was a generous gift from Dr Randy Schekman (University of Berkeley, USA). Polyclonal antibodies against Vma8p and Vma5p were raised in guinea pigs and used at a dilution of 1:1000. The antibody detection system (ECL) was from Amersham. Western blots were performed as previously described (Cohen et al., 1999).

Membrane preparations and protein subcellular fractionation

Whole-cell extracts from the strains were prepared as described by Lyons and Nelson (1984) with several modifications. Briefly, yeast cells (20 ml) were grown to late logarithmic phase, centrifuged and washed once with water. Cells were resuspended in 0.45 ml water. Sodium hydroxide and 2-mercaptoethanol were added to a final concentration of 0.2 mol l^{-1} and 0.5 %, respectively. The suspension was placed on ice for 20 min, then 0.125 ml of dissociation buffer (2% SDS, 80 mmol l^{-1} Tris-HCl, pH 6.8, 1% 2-mercaptoethanol, 10 % glycerol and 0.01 % Bromophenol Blue) was added and

adjusted immediately with HCl to pH 7.5–8. The proteins were extracted for 1 h at room temperature and insoluble material was removed by centrifugation in an Eppendorf centrifuge (18,000 ***g***) at room temperature for 10 min.

For membrane preparation, yeast cells were grown in 500 ml YPD medium (pH 5.5) to A_{600}=1.0. The suspension was centrifuged at 3000 ***g*** for 5 min and the pellet was washed once with water and again with 1 mol l^{-1} sorbitol. The cell wall was digested by 2.5 U zymolyase in 10 ml solution containing 10 mmol l^{-1} Hepes, pH 7.5, and 1 mol l^{-1} sorbitol. After 30 min incubation at 30 °C, the suspension was centrifuged in 15 ml Corex tubes at 3000 ***g*** for 5 min. Glass beads (1 ml) were added to the pellet, together with 1 ml of a solution containing 30 mmol l^{-1} Mops, pH 7.0, 10 μl protease inhibitor cocktail (Sigma), 1 mmol l^{-1} phenylmethylsulfonyl fluoride (PMSF), 1 mmol l^{-1} EDTA and 1 mmol l^{-1} EGTA. The suspension was vortexed five times for 30 s each with incubation on ice for 30 s inbetween. The solution was removed from the glass beads and placed in a fresh Corex tube for centrifugation at 1000 ***g*** for 5 min, forming a pellet containing the cell debris and nuclei. The supernatant was centrifuged at 115,000 ***g*** for 30 min and the pellet was suspended in 0.3–0.5 ml of solution containing 10 mmol l^{-1} Tris-Cl, pH 7.5, 1 mmol l^{-1} EDTA, 2 mmol l^{-1} dithiothreitol (DTT), 25 % glycerol, and stored as the membrane fraction at –80 °C. Sucrose gradients were also used to estimate the relative density of various membrane fractions. The gradients (20 %–60 % sucrose) were made as described by Lupashin et al. (1997), and were centrifuged in a Beckman SW-40 rotor for 14 h at 150,000 ***g***.

Differential centrifugation analysis and sucrose gradient fractionation of Golgi membranes were performed as previously described (Graham et al., 1994; Graham and Krasnov, 1995). Briefly, spheroplasts (300 A_{600} units) obtained by zymolyase treatment (0.125 mg ml^{-1} in 50 mmol l^{-1} Tris-HCl, pH 7.5, 1.4 mol l^{-1} sorbitol, 40 mmol l^{-1} 2-mercaptoethanol) were lysed by sevenfold dilution in hypo-osmotic buffer (0.1 mol l^{-1} sorbitol, 10 mmol l^{-1} TEA, pH 7.5, 1 mmol l^{-1} EDTA) followed by Dounce homogenisation (25 strokes). The lysate was centrifuged at 1000 ***g*** for 6 min to generate P1 (pellet) and S1 (supernatant) fractions, and the latter was centrifuged at 13,000 ***g*** to generate P13 and S13 fractions. The S13 fraction was layered onto a two-step sucrose cushion consisting of 1 ml of 66 % sucrose and 1 ml of 20 % sucrose, then centrifuged in a Beckman SW-40 rotor at 120,000 ***g*** for 2 h at 4 °C. The membranes present at the 20%–66 % sucrose interface (P120) were collected in a volume of approx. 1.2 ml and adjusted to approx. 48 % sucrose using a 66 % sucrose solution. The membrane sample (1.5 ml) was layered on top of a 60 % sucrose cushion (0.5 ml) and a sucrose step gradient consisting of 47.5 % (1.5 ml), 45 % (1.0 ml), 42 % (2.0 ml), 40 % (2.0 ml), 38 % (1.0 ml), 36 % (1.0 ml) and 32 % (1.5 ml) sucrose was layered on top of the sample. All sucrose solutions were prepared in 10 mmol l^{-1} Na-Hepes, pH 7.5. The gradients were centrifuged in an SW-40 rotor at 31,000 ***g*** for 17 h at 4 °C. Fifteen fractions (approx. 0.7 ml) were collected, starting from the bottom of the gradient. The proteins from each fraction were precipitated by addition of 0.13 ml of 5× SDS-sample buffer and 1.0 ml of ice-cold ethanol. After incubation on ice for 30 min, the samples were centrifuged at 18,000 ***g*** for 30 min at 4 °C. After aspiration of the supernatants, the pellets were resuspended in 0.05 ml of SDS-sample buffer and stored at –20 °C.

Preparation of yeast vacuoles

For preparation of vacuoles, cells were grown in YPD medium adjusted to pH 5.5 with HCl and harvested at a cell density of about 0.8 A_{600} units. Vacuolar membranes were prepared according to the method of Uchida et al. (1985), except that the 8 % Ficoll gradient purification step was omitted, the homogenization buffer contained no magnesium and the vacuoles were washed only once with the EDTA buffer (10 mmol l^{-1} Tris-HCl, pH 7.5, 1 mmol l^{-1} EDTA, 2 mmol l^{-1} DTT). ATP-dependent proton uptake activity was assayed by following the absorbency changes of Acridine Orange at 490–540 nm as previously described (Supek et al., 1994). The reaction mixture (1 ml) contained 20 mmol l^{-1} Mops-Tris, pH 7, 15 mmol l^{-1} KCl, 135 mmol l^{-1} NaCl and 15 μmol l^{-1} Acridine Orange. Isolated yeast vacuoles (10–30 μg) were added to the reaction mixture followed by 10 μl of 0.1 mol l^{-1} MgATP. The reaction was terminated by the addition of 1 μl of 1 mmol l^{-1} carbonyl cyanide *p*-(trifluoromethoxy)phenyl-hydrazone (FCCP).

Vacuole staining with fluorescent probes

For FM4-64 vacuolar staining, cells were grown in YPD to A_{600}=0.8–1.6. Cells (20–40 A_{600} units ml^{-1} in YPD medium) were incubated on ice for 30 min with 30 μmol l^{-1} FM4-64 dye (Molecular Probes Inc.), washed once with YPD and incubated for 60 min for steady-state experiments as described (Vida and Emr, 1995).

For Quinacrine staining, yeast cells were grown in YPD to A_{600}=0.8. The cells were cooled on ice for 5 min and 1 ml of cell suspension was sedimented by centrifugation and resuspended in 100 μl YPD containing 100 mmol l^{-1} Hepes, pH 7.6, and 200 μmol l^{-1} freshly prepared Quinacrine. The suspension was incubated for 5–10 min at 30 °C and cooled on ice for 5 min. The cells were sedimented by centrifugation and resuspended in 1 ml 100 mmol l^{-1} Hepes, pH 7.6, 2 % glucose. The cells were washed twice with the same cold buffer and resuspended in 0.1 ml of the same solution. 4 μl of the cell suspension was mixed on the microscope slide with 4 μl of 1 % low-melting agarose kept at about 45 °C and covered with a glass cover. The cells were examined using a Zeiss LSM510 confocal laser microscope. Fluorescence profiles were generated using a Zeiss LSM Image browser.

For LysoSensor Green DND-189 staining (Molecular Probes Inc), all strains were grown at 30 °C to A_{600}=0.7–1. Cells were harvested and washed with uptake buffer (YPD containing 100 mmol l^{-1} Hepes, pH 7.6). The cell pellets were resuspended at a concentration of 15 A_{600} units ml^{-1} in uptake buffer and dye was added to a final concentration of 4 μmol l^{-1} from a stock solution of 1 mmol l^{-1} in DMSO. Cells were then

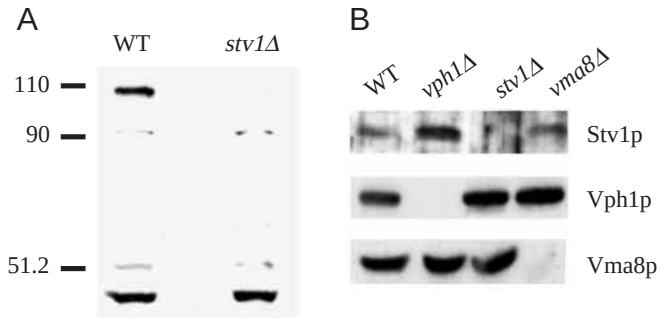

Fig. 1. Null mutation of *VPH1* causes overexpression of Stv1p. (A) Western analysis of whole cell extracts of wild type (WT) and *stv1Δ* mutants. Stv1p is absent from the *stv1Δ* strain. Some non-specific bands are labeled by the polyclonal antibody. The positions of marker proteins (kDa) are shown. (B) Western analysis of wild type, *vph1Δ*, *stv1Δ* and *vma8Δ* strains. Whole cell extracts from the strains were prepared as described in Materials and methods. Total cellular proteins (20 μg per lane) were subjected to SDS-PAGE and immunoblotted with antibodies against Stv1p, Vph1p and Vma8p.

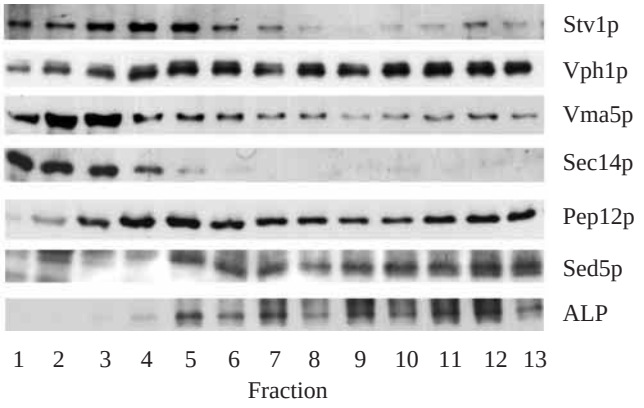

Fig. 2. Vph1p and Stv1p cofractionate with membranes containing the Golgi-endosome and vacuolar markers. An enriched Golgi membrane fractionation was prepared from the wild type as described in Materials and methods. Western analysis of these fractions with antibodies against Vph1p, Stv1p, Vma5p, Sec14p (a late Golgi protein), Sed5p (a *cis*-Golgi protein), Pep12p (an endosomal marker) and ALP (vacuolar membrane marker) is shown. Fraction numbers are indicated at the bottom.

incubated for 5 min at 30 °C and washed once with the same buffer. Cell pellets were resuspended in fresh YPD, pH 7.6, at 15 A_{600} units ml^{-1}, placed on standard slides with low-melting agarose and photographed immediately after staining. The samples were viewed using a confocal laser scanning microscope (Zeiss) equipped with an Argon 458 nm laser and a C-Apochromat 63× water immersion objective. A LP505 filter was used for LysoSensor Green DND-189 fluorescence. The images were recorded, merged and processed using the Zeiss LSM Image browser.

Results

Stv1p and Vph1p cell localization

To analyze the intracellular localization of Stv1p, we prepared a rabbit polyclonal antiserum against a bacterially expressed fragment of Stv1p (amino acid residues 231-436; see Materials and methods). Fig. 1A shows that affinity-purified anti-Stv1p antibodies recognized a protein of approx. 110 kDa on an immunoblot of a wild-type cell lysate, as was previously reported (Manolson et al., 1994). This protein was not present in the *stv1Δ* cell lysate and was found in greater abundance in the *vph1Δ* strain than in wild type (Fig. 1B). These results suggest that Stv1p compensates for the loss of Vph1p in the *vph1Δ* strain by increasing the stability or overproduction of Stv1p in that strain, since there are no differences in the m-RNA levels for either subunit a isoform following disruption of one of them (Manolson et al., 1994).

Immunolocalization studies of Vph1p and Stv1p in yeast suggested that Vph1p is localized in the central vacuole, whereas Stv1p is localized in some other intracellular compartments, possibly the Golgi or endosomes (Manolson et al., 1994). Several studies showed that V-ATPase is present along the Golgi complex (Moriyama and Nelson, 1989; Ying et al., 2000; Grunow et al., 1999). Subcellular fractionation of the Golgi membranes using the technique of Graham and Krasnov (1995) was used to determine the location of the Stv1p subunit more precisely. This technique separates the vacuoles more efficiently and allows better detection of the V-ATPase complex in the different Golgi and endosomal fractions. The cell membranes were applied to the bottom of a sucrose gradient and centrifuged to equilibrium. Fractions were collected from the bottom and probed with antibodies against Stv1p, Vph1p, Pep12p, Sec14p and Sed5p. Sed5p is the marker for early Golgi compartments, Sec14p for the late Golgi vesicles and Pep12p for endosomes. In the fractionation profile shown in Fig. 2, Vph1p and Stv1p were broadly distributed throughout the gradient. Furthermore, the Vph1p profile matches that of the Pep12p profile, suggesting an endosomal distribution on the gradient. ALP (vacuolar membrane protein) marks the vacuolar membrane contamination. Stv1p is located in two peaks along the gradient. The first peak (fractions 3–5) coincides slightly better than Vph1p with the Sec 14p (*trans*-Golgi) distribution, and the second peak (fractions 12,13) matches the broad profiles of Pep12p and Sed5p (Fig. 2). We also found that the V_1 subunit, Vma5p, peaked in the first four fractions. The peak of Vma5p overlapped mostly with that of Sec14p, raising the possibility that the assembled V-ATPase complex present in a late Golgi compartment is more stable. A similar distribution was also observed for Vma8p, another V_1 subunit (not shown). Assuming that the amount of assembled V-ATPase is an indicator of its ATPase activity, these results support previous reports that acidification develops along the Golgi complex and is maximal in the *trans*-Golgi compartment (Llopis et al., 1998; Schapiro and Grinstein, 2000). Fractionation in yeast does not yield clean separation of compartments, so it is difficult to draw exact conclusions about localization. Assuming that the two subunit a isoforms are in

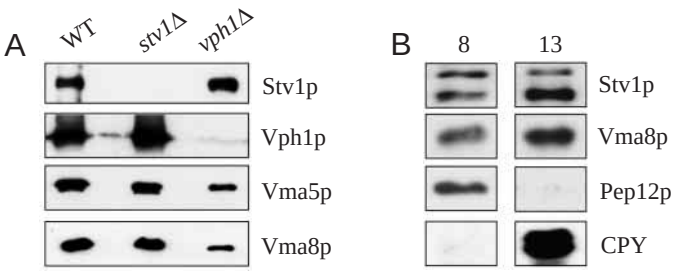

Fig. 3. *vph1Δ* strain has an assembled V-ATPase complex in the vacuole. (A) Yeast vacuoles were isolated from wild type (WT), *vph1Δ* and *stv1Δ* strains as described in Materials and methods. Samples containing 10 μg protein were applied in each lane. Following electrotransfer, the nitrocellulose membranes were decorated with the indicated antibodies. (B) Isolated yeast vacuoles of *vph1Δ* cells (0.5 ml) were placed on top of 20%–60 % sucrose gradients in a buffer containing 20 mmol l^{-1} Mops, pH 7.2, 1 mmol l^{-1} EDTA. The gradients were centrifuged in an SW-40 rotor at 150,000 ***g*** for 14 h. The first 13 fractions collected from the bottom of the tube were assayed by immunoblotting for the V-ATPase with Vma8p and Stv1p, an endosomal t-SNARE Pep12p, and a vacuolar protein CPY. In both fractions 8 and 13, the degradation product of Stv1p, as reported earlier (Manolson et al., 1994) is visible.

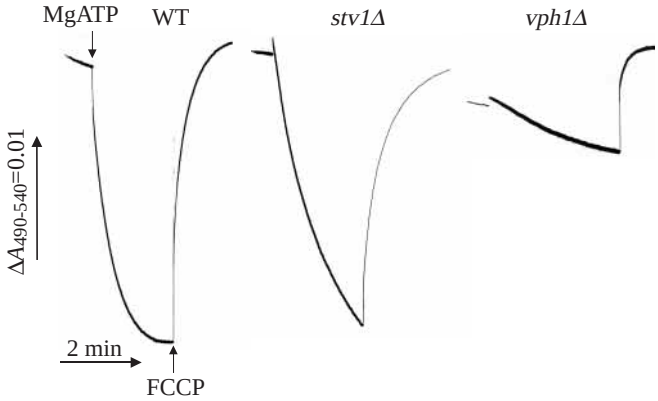

Fig. 4. Acridine Orange uptake into isolated vacuoles from *stv1Δ* and *vph1Δ* strains shows diminished activity. Yeast vacuoles were isolated by Ficoll gradient centrifugation and adjusted to a protein concentration of 2 mg ml^{-1} (Uchida et al., 1985). ATP-dependent proton uptake was measured by following Acridine Orange absorption changes (Δ*A*) at 491–540 nm. Vacuoles containing 10 μg of protein were assayed in each sample. Where indicated by an arrow, 10 μl of 0.1 mol l^{-1} MgATP or 1 μl of 1 mmol l^{-1} carbonyl cyanide *p*-(trifluoromethoxy)phenylhydrazone (FCCP) was added.

separate complexes, and that this western profile represents assembled and unassembled proteins, we can cautiously say that from the relative amounts, at least in fraction 3, Stv1p is the V-ATPase isoform in the Golgi complex.

Stv1p localization in vph1Δ *strain*

It was proposed that Stv1p does not normally reside on the vacuolar membrane in wild-type cells, and only overexpressed Stv1p-HA in *vph1Δ/stv1Δ* and *vph1Δ* strains could be found in the vacuolar membrane (Manolson et al., 1994; Kawasaki-Nishi et al., 2001). On the other hand, detectable levels of Vma1p and Vma2p were found to be associated with vacuoles from the *vph1Δ* strain (Manolson et al., 1992). Our antibody revealed that purified vacuoles from wild-type cells also contain Stv1p. Fig. 3A shows a western analysis of purified vacuoles from wild-type, *stv1Δ* and *vph1Δ* probed with antibodies against Stv1p, Vph1p, Vma5p and Vma8p. Stv1p is detected in vacuolar membranes from the wild-type and *vph1Δ* cells. These data also demonstrate that the level of Stv1p in the *vph1Δ* mutant strain increased in comparison to the wild-type strain, as was found for Vph1 in *stv1Δ* mutant (Fig. 1B). On the other hand, the amount of V-ATPase complex in the *vph1Δ* was reduced significantly (based on amounts of the V_1 subunits of V-ATPase, Vma5p and Vma8p present in those vacuolar membranes) as compared to the wild type.

Although vacuolar membranes isolated from the *vph1Δ* strain contained an evidently assembled V-ATPase complex (see Fig. 3A), it was still possible that other V-ATPase-containing membranes also contaminated the vacuoles of *vph1Δ* strain and wild-type. We could detect Golgi and endosomal proteins in isolated vacuoles with antibodies against Sec14p and Pep12p, respectively (data not shown). Fig. 3B depicts two fractions of the gradient (8 and 13) showing, respectively, endosomal and intact vacuolar fractions, which were obtained from a sucrose gradient fractionation of *vph1Δ* strain, decorated with antibody against CPY (a soluble vacuolar marker), Pep12p antibody (an endosomal marker), and Vma8p and Stv1p antibodies. Fraction 8 represents the peak of the endosomal fractions and fraction 13 the peak of the vacuolar fractions. CPY is a vacuolar-soluble protein, so we also probed both fractions with antibody against ALP, a resident of the vacuolar membrane, that was present throughout the gradient (not shown). These data are in agreement with the assumption that an assembled V-ATPase complex is present in the vacuole in *vph1Δ* strain with no detectable endosomal contamination.

V-ATPase proton uptake activity in vph1Δ *and* stv1Δ *strains*

Previous work has demonstrated that vacuoles of a *vph1Δ* mutant with neutral lumenal pH do not accumulate Quinacrine and have no detectable bafilomycin A_1-sensitive V-ATPase activity (Manolson et al., 1994). Because we showed that small amounts of assembled V-ATPase complex are present in vacuoles from our *vph1Δ* strain, it was of interest to assess their proton pumping activity. Fig. 4 shows the ATP-dependent proton uptake activity of vacuoles isolated from wild-type, *stv1Δ* and *vph1Δ* strains. The ATP-dependent proton uptake activity from the *vph1Δ* mutant (26 nmol min^{-1} mg^{-1}) was 30-fold less than the specific activity of wild-type (817 nmol min^{-1} mg^{-1}), but nevertheless measurable. This explains the observation that Quinacrine fluorescence, which is dependent on higher proton concentrations, was not observed in the *vph1Δ* strain. Strains that overexpress Stv1p showed a marked reduction in the assembled V-ATPase

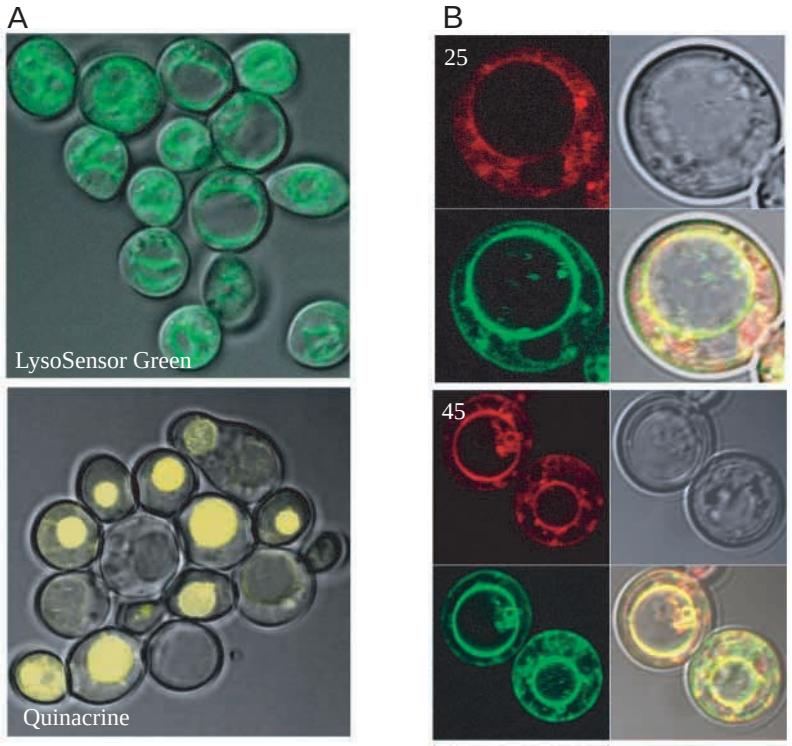

Fig. 5. LysoSensor Green DND-189 is a vital dye that fluoresces in the acidic compartments of the yeast cell. (A) Comparison of LysoSensor Green DND-189 and Quinacrine staining. Wild-type cells were stained separately with LysoSensor Green DND-189 and Quinacrine as described in Materials and methods. (B) Wild-type cells were incubated at 0 °C for 30 min with 30 μmol l^{-1} FM 4-64 in YPD medium buffered with 100 mmol l^{-1} Hepes, pH 7.6. The cells were harvested by centrifugation, washed once with the same buffer, and resuspended in 0.35 ml of fresh medium containing 4 μmol l^{-1} LysoSensor Green DND-189. Cells were then incubated for 5 min, harvested by centrifugation, washed and resuspended in YPD medium. Portions were removed for microscopy and photographed at 25 min (top) and 45 min (bottom). Top left of each panel, FM 4-64 fluorescence; top right, the same cells in visible light; bottom left, LysoSensor Green DND-189 fluorescence; bottom right, the double-labeled image. The images were recorded, merged and processed using the Zeiss LSM Image Browser.

complex, even though there were appreciable amounts of Stv1p in the vacuolar membrane (Kawasaki-Nishi et al., 2001). It appears that deletion of the *VPH1* gene results in naturally overexpressed Stv1p in vacuolar membranes (Figs 1B, 3A). These results also suggest that the compensation of a *vph1Δ* mutant by Stv1p is only partial.

As a control for V-ATPase activity we isolated vacuoles from a *stv1Δ* strain. Surprisingly, the initial rate of V-ATPase activity in these vacuoles was diminished by 40–50 % (see Fig. 4). This highly reproducible result led us to do a more careful analysis of the amounts of V_1 subunits upon the vacuolar membranes in this strain, which are more indicative of the enzyme's activity. A reduction in Vma5p and Vma8p is apparent on western blot analysis (Fig. 3A), whereas the Vph1p level is slightly higher than in wild type. This pattern suggests that in wild type the Stv1p in its post-Golgi location plays a role in facilitating the assembly process of the holoenzyme in the vacuolar membrane.

LysoSensor Green DND-189 staining of V-ATPase null mutants

LysoSensor Green DND-189 is an acidotropic probe that accumulates in the membranes of acidic organelles as a result of protonation. It was used to investigate the acidic compartments in cultured cerebellar granule cells and plant tissue (Cousin and Nicholls, 1997; Guttenberger, 2000). We used this dye to stain the acidic compartments of yeast (see Materials and methods). The dye labeled the vacuolar membranes of wild-type cells in less than 5 min, and the signal remained stable for more than 1 h. The staining is more efficient than with Quinacrine, as shown in Fig. 5A, which shows parallel labeling of wild-type cells with LysoSensor Green DND-189 and Quinacrine (a vital dye for the vacuolar lumen). LysoSensor Green detects acidic vacuoles in almost 100 % of the stained cells. The vacuolar staining was confirmed by double labeling with FM4-64 lipophilic styryl dye, which selectively stains endocytic compartments and yeast vacuolar membranes. Fig. 5B shows double-staining images at different intervals. After 25 min the green staining of the vacuolar membrane is clearly visible, and the red staining by FM 4-64 is concentrated mainly in cytoplasmic vesicles, which may correspond to endosomes (Vida and Emr, 1995). Some of these vesicles are definitely not stained by LysoSensor Green; conversely some vesicles are stained by LysoSensor Green but not by FM4-64. After 45 min the staining of the vacuolar membrane by the FM4-64 is almost complete. Double staining of the vacuolar ring (Fig. 5B) also demonstrates that LysoSensor Green DND-189 is an efficient dye for the staining of acidic compartments in yeast.

LysoSensor Green was used to examine vacuolar membrane staining of wild type, *vph1Δ* and *stv1Δ* mutants and the double mutant *vph1Δ/stv1Δ* cells. The vacuolar membrane was stained normally in wild-type cells, but no staining was observed in the double mutant *vph1Δ/stv1Δ*, other V-ATPase null mutants (Fig. 6), or in wild-type cells treated with the specific V-ATPase inhibitor concanamycin A (not shown). LysoSensor Green staining and V-ATPase activity are correlated in the *vtc1Δ* mutant, which was shown to have diminished V-ATPase activity *in vitro* (Cohen et al., 1999), while its staining with the vital dye was much less intense than that of the wild-type cells (not shown). Our results obtained with the *stv1Δ* mutant, which grows well in YPD medium, pH 7.5, showed that the intensity

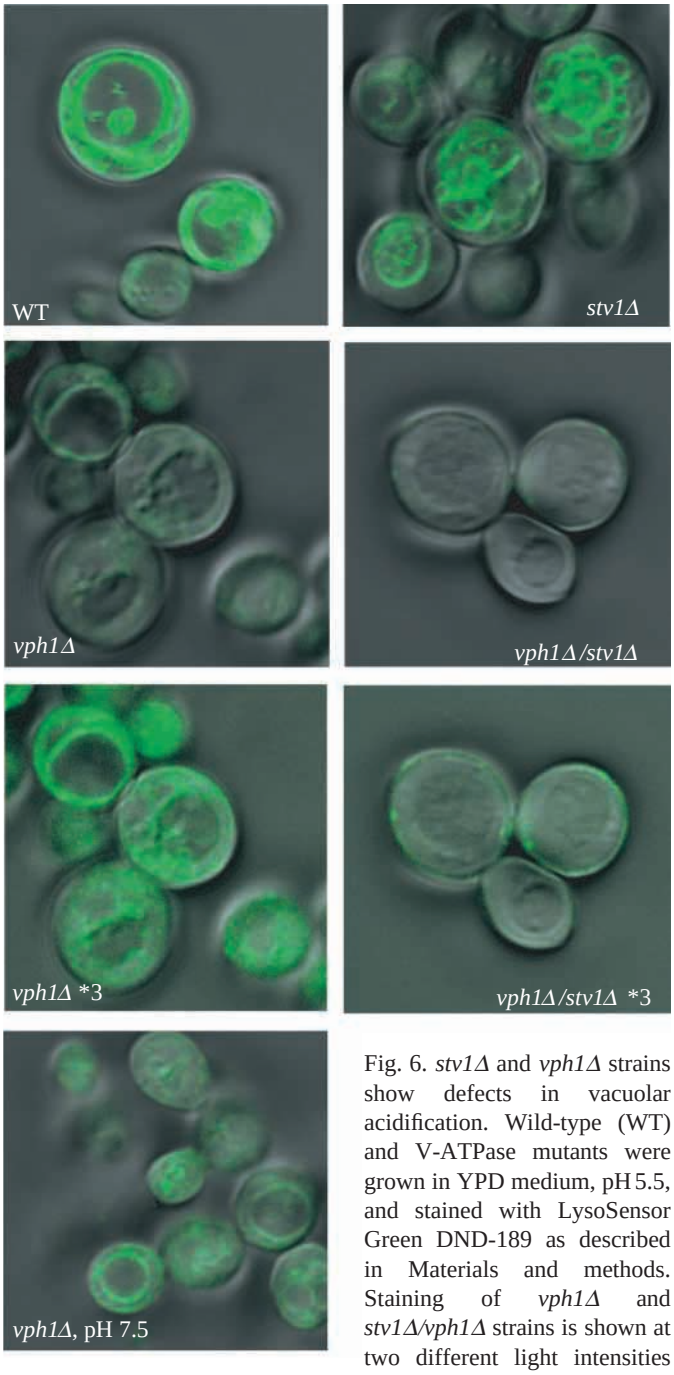

Fig. 6. *stv1Δ* and *vph1Δ* strains show defects in vacuolar acidification. Wild-type (WT) and V-ATPase mutants were grown in YPD medium, pH 5.5, and stained with LysoSensor Green DND-189 as described in Materials and methods. Staining of *vph1Δ* and *stv1Δ/vph1Δ* strains is shown at two different light intensities (*3 is triple intensity). The panel below shows staining of *vph1Δ* grown in YPD buffered at pH 7.5.

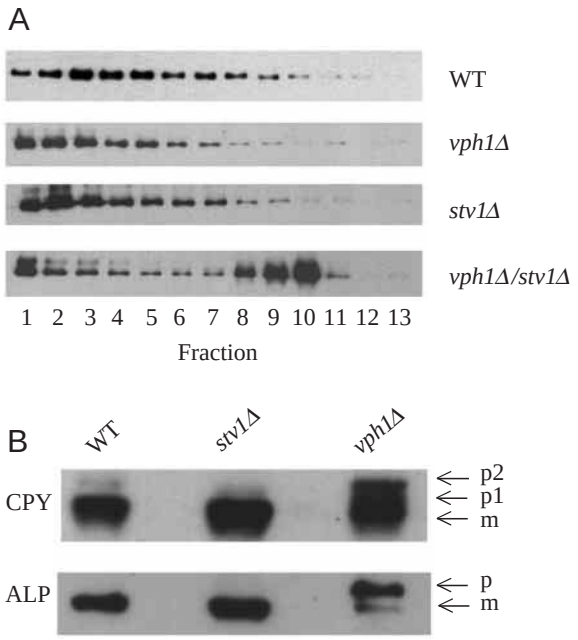

Fig. 7. Differential effect of *stv1Δ* and *vph1Δ* mutants on Pma1p sorting and CPY and ALP processing. (A) Sucrose density gradients of whole cell extracts from wild type (WT), *stv1Δ, vph1Δ* and *stv1Δ/vph1Δ* strains were prepared as described in Materials and methods. The location of Pma1p was determined by immunoblot analysis with polyclonal antibody against purified Pma1p. Fraction numbers are indicated at the bottom. (B) Western analysis of vacuoles isolated from wild type, *stv1Δ* and *vph1Δ* strains by Ficoll gradient centrifugation and adjusted to a protein concentration of 2 mg ml^{-1} with antibodies against CPY and ALP. p, precursor of ALP; p1 and p2, precursors of CPY; m, mature form of the protein.

of the vacuolar staining was lower than in the wild type (Fig. 6). This observation is in agreement with the data in Fig. 4, which demonstrate reduced V-ATPase activity in the *stv1Δ* strain. Interesting results were observed in *vph1Δ* cells. Half of the cells were weakly stained and the others, when the signal was intensified, showed a clear difference between *vph1Δ* and the double mutant in vacuolar staining (Fig. 6). This observation suggests that, in *vph1Δ* cells, Stv1p might reach the vacuolar membrane, as also indicated by western analysis (Fig. 3). Moreover, when grown on a medium buffered at pH 7.5, the staining of vacuoles in the *vph1Δ* cells is intensified (Fig. 6).

Protein sorting in vph1Δ and stv1Δ mutants

We recently investigated the effect of vacuolar ATPase null mutations on the targeting of the plasma membrane H^+-ATPase (Pma1p) through the secretory pathway (Perzov et al., 2000). We showed that the amounts of Pma1p in the plasma membranes of V-ATPase-depleted mutants were markedly reduced, and a large amount of the protein was accumulated in the ER-Golgi in a non-active form. If Stv1p and Vph1p are part of separate V-ATPase complexes in distinct compartments, we might expect differential effects on Pma1p distribution in both mutants. We therefore performed sucrose gradient fractionation on total membranes prepared from the wild-type, *vph1Δ, stv1Δ* and *vph1Δ/stv1Δ* strains. As shown in Fig. 7A, the distribution of Pma1p in the sucrose gradient fractions of the membrane preparation was not altered in *stv1Δ* and *vph1Δ* strains, but was altered in the *vph1Δ/stv1Δ* null mutant, as is usually observed in other null V-ATPase mutants. These results indicate that only complete inactivation of the V-ATPase in all cellular compartments leads to redistribution of Pma1p. In contrast, we observed defects in processing of

vacuolar hydrolyses in *vph1Δ* cells, while in the *stv1Δ* strain the vacuolar proteins mature as in the wild type (Fig. 7B).

Effect of V-ATPase null mutations on FM4-64 internalization

FM4-64 is a fluorescent lipophilic dye, which serves as a marker for endocytosis and has been used for this purpose in yeast (Vida and Emr, 1995). The dye is initially incorporated into the plasma membrane and, through endocytosis, reaches and accumulates in the vacuolar membrane. It has been suggested that the acidification of endocytic organelles by V-ATPase is essential for endosomal trafficking in mammalian cells (Clague, 1998). We used FM4-64 dye to investigate the role of acidification in endosomal trafficking in yeast. The wild-type and null V-ATPase strains were stained with FM4-64 and the localization of the dye recorded after 20, 40, 60 and 90 min. Fig. 8A shows that, in the wild-type strain, the dye reaches the vacuole after 20 min and stains it strongly after 40 min. Vacuolar staining in the *vma3Δ* mutant is inhibited, and after 60 min the cells do not even show the vacuolar staining which the wild-type cells do after 20 min. After 60 min of internalization, the dye stained vacuolar membranes only in the wild type, whereas in the *vma3Δ* mutant, *vph1Δ/stv1Δ* cells or other null V-ATPase mutants, much of the internalized dye only reaches vesicular intermediates in the cytoplasm and levels do not change much during this time. Only after 90 min does some of the dye reach the vacuolar membrane. Fig. 8B summarizes the staining data obtained with *vph1Δ* and *stv1Δ* cells. The transport of the dye to the vacuole in *vph1Δ* cells resembles that in null mutants, but slight staining of the vacuolar membranes is observed in some cells (Fig. 8B). In *stv1Δ* cells, FM4-64 reached the vacuolar membrane with kinetics similar to the wild type, but a mix of fragmented vacuoles was observed very frequently (a similar vacuolar pattern was obtained by staining the *stv1Δ* strain with LysoSensor Green dye, see Fig. 6). Fragmented vacuoles are a component of the phenotype in the *stv1Δ* strain.

Fragmented vacuoles and no defect in endocytic delivery of the dye to the vacuole were also detected in *vps1Δ* cells (Raymond et al., 1992; Nothwehr et al., 1995; Vida and Emr, 1995). Vps1p is a dynamin-like protein required for formation of endosome-bound vesicles from the Golgi, and in *vps1Δ* mutants endosomal-bound transport is diverted to the cell surface (Nothwehr et al., 1995).

These data indicate that the null V-ATPase mutants, as well as the *vph1Δ* mutant, markedly slow down the endocytic process in the yeast cells. To test this further, we stained the wild-type strain in the presence of 3 μmol l^{-1} concanamycin A, a specific inhibitor of V-ATPase. Fig. 9 shows that the drug inhibited the internalization of FM4-64, making the wild type similar to the stained V-ATPase null mutant: endosomal-like structures near the vacuolar membrane are stained, but the stain does not reach the vacuole membrane.

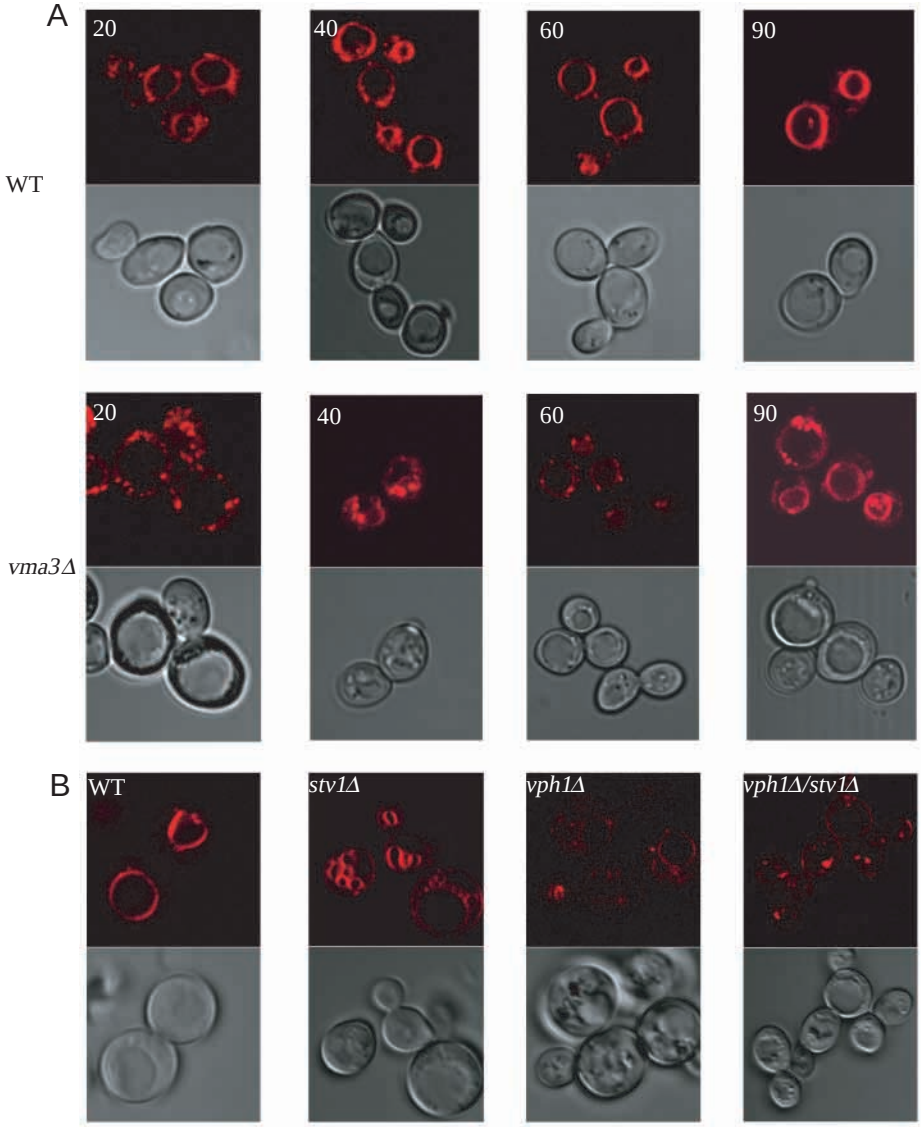

Fig. 8. Endocytosis of the fluorescent endocytic marker FM 4-64 to vacuolar membranes is slowed down in V-ATPase null mutants. (A) Wild-type (WT) and *vma3Δ* cells were stained with FM 4-64 as described in Materials and methods. Samples were removed for microscopy after staining for the indicated times (min), in order to monitor the internalization kinetics of the dye. (B) The indicated strains were stained with FM 4-64 and photographed after a 60 min chase in YPD medium. Top panels show FM 4-64 fluorescence; bottom panels show visible light images of the same cells.

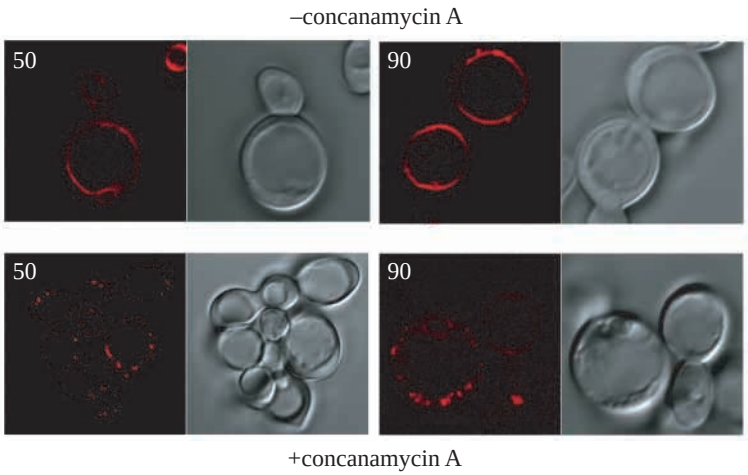

Fig. 9. Concanamycin A inhibits endocytosis in wild-type cells. Wild-type cells were treated (+) or not (–) for 20 min with 3 μmol l^{-1} concanamycin A (dissolved in DMSO solution) before staining with FM 4-64, according to the standard procedure. Staining images were visualized at 50 min and 90 min. Left panels, FM 4-64 fluorescence; right panels, visible light images of the same cells.

Discussion

Vacuolar H^+-ATPase generates the energy and appropriate pH for the various compartments of the vacuolar system of the cell (Stevens and Forgac, 1997; Nelson and Harvey, 1999). In many plant and animal species, the various subunits of V-ATPase have numerous isoforms (Futai et al., 2000). It is believed that each isoform resides in a different compartment and may even play a role in targeting the whole complex into this compartment. In yeast, all subunits except for subunit a are encoded by a single gene, so the study of Vph1p and Stv1p is interesting because subunit a may have a role in targeting the complex to specific organelles, as well as in modulating the activity of the enzyme. We set out to describe the phenotype of the *STV1* null mutant. Previously Stv1p was assigned to Golgi and/or endosome compartments by immunofluorescent staining (Manolson et al., 1994), correlated with its Golgi retention motive FXFXD; however, no specific features were found for its null mutant. This could be explained by redundancy or by lack of methods to discover the phenotype. First, we have to establish that Stv1p and Vph1p subunits are part of different V-ATPase complexes. This was proposed following work in which Stv1p was first described (Manolson et al., 1994) but no direct proof was available. We tried to immunoprecipitate the V-ATPase membrane complex (V_o) from isolated yeast membranes with Vph1p commercial monoclonal antibody 10D7 (which recognizes its epitope only after V_1 dissociation). We detected Vma3p in the immunoprecipitate, but did not detect any Stv1p with our polyclonal antibody for the Stv1p that was found in the supernatant (data not shown).

V-ATPase is present along the secretory pathway and plays a central role in its proper function, especially in the Golgi complex (Moriyama and Nelson, 1989; Grunow et al., 1999; Ying et al., 2000; Schoonderwoert et al., 2000). To demonstrate the subcellular location of Stv1p we used a Golgi fractionation method (Graham and Krasnov, 1995), which separates between *cis*- and *trans*-Golgi. Using this gradient we found that Stv1p and Vph1p in the wild type showed different profiles: Vph1p exhibited mainly an endosomal pattern, and was probably on its way to the vacuole, whereas Stv1p peaked nearer to *trans*-Golgi. V_1 subunits Vma5p and Vma8p showed a main peak in *trans*-Golgi, which might indicate that this location has the most stable V-ATPase complex. The pH along the secretory pathway falls from the ER through Golgi and reaches maximum acidity in lysosomes (Grabe and Oster, 2001; Llopis et al., 1998). In the Golgi complex the *trans*-Golgi is the most acidic compartment, which is in good agreement with the high levels of V-ATPase amounts described above.

By disrupting one of the a subunits we can demonstrate that the other partially compensates for the lack of its counterpart. Therefore, both mutants of one isoform lack some features of the null V-ATPase mutant growth profile. However, it may be that the ability of Stv1p to compensate for the lack of Vph1p in the *vph1Δ* mutant is at much lower efficiency (Figs 3, 4) because it is less stable in the vacuolar membrane (Kawasaki-Nishi et al., 2001). This is seen in the higher rate of growth at pH 7.5, as well as in the processing of the vacuolar proteins ALP and CPY (see Fig. 7B) when compared to *vph1Δ*. We do not see the same results for the reciprocal mutant (*stv1Δ*), which might indicate that Vph1p functions normally in place of Stv1p (Fig. 7B). It was therefore interesting to see that the specific activity of proton pumping by V-ATPase in vacuoles isolated from the *stv1Δ* mutant was diminished in comparison to the wild-type strain. Even though Vph1p itself is overexpressed in the vacuolar membrane in the *stv1Δ* mutant (Figs 3A, 4), there is less holoenzyme present in it, hence the decrease in activity. Stv1p is therefore not redundant in the wild type. The complex containing it has a role in its proper functioning, as does the complex containing the Vph1p.

The same results were obtained by *in vivo* staining of these yeast strains with a fluorescent pH indicator, LysoSensor Green. Examination of stained yeast cells revealed residual staining in vacuolar membranes, in the Vph1p null mutant (but not in the double mutant), which correlates with the small but measurable H^+ translocating activity of V-ATPase in the vacuoles of the *vph1Δ* mutant (Fig. 6).

The relationship between V-ATPase function and the endocytosis processes is intriguing. On the one hand, endocytosis is responsible for the viability of yeast V-ATPase null mutants, while on the other, some of the endocytosis mutants were described to have a very similar phenotype to the V-ATPase null mutant (Munn and Riezman, 1994; D'Hondt et al., 2000; Yoshida and Anraku, 2000). The acidification of endosomal compartments due to V-ATPase activity and its relation to endocytic processes, e.g. ligand-receptor dissociation during receptor-mediated endocytosis, is

well-established in mammalian cells (Mellman et al., 1986). Other studies showed that endosomal carrier vesicle formation, as well as transfer between late endosomes and lysosomes, are pH-sensitive processes inhibited by the specific V-ATPase inhibitor bafilomycin A (Clague et al., 1994; van Weert et al., 1995; van Deurs et al., 1996). In yeast, the same relationship has yet to be demonstrated. The FM4-64 dye staining of yeast cells was used to visualize endocytosis *in vivo* (Vida and Emr, 1995), and to stain the V-ATPase null mutant in comparison to the wild-type strain. We found inhibition of FM 4-64 internalization in the V-ATPase null mutants. After treatment for 60 min, during which time all the dye concentrated in the vacuolar membrane in the wild type, much of the internalized dye in the mutants only reached endosomes surrounding the vacuolar membrane. We could mimic the mutant in the wild-type cells by addition of concanamycin A, which specifically inhibits V-ATPase activity (Fig. 9).

Since the staining kinetics of this dye are used as a measure for endocytosis, we conclude that V-ATPase mutants inhibit endocytosis in yeast as well. We see that the staining of the plasma membrane (not shown) and of the cytoplasmic vesicles, presumably endosomes, is similar for both the wild type and null V-ATPase mutants. However, the final step of internalization of the dye in the vacuolar membrane is markedly dependent on proper V-ATPase functioning. FM4-64 was used to examine whether the *stv1Δ* or *vph1Δ* might have a phenotype in endocytosis. Fig. 8 shows that the Vph1p null mutant displays the double-mutant phenotype, while the Stv1p null mutant has similar staining kinetics to wild type but exhibits prevalent vacuolar localization.

As expected for such a fundamental enzyme, its null mutation, if viable, should affect a vital pathway or pathways of the cell. We conclude that the V-ATPase function is to determine the pH conditions, not only in the lumen of their respective organelles, but also in processes involved in intervesicular activities connected with membrane fusion. A similar conclusion was reached by Ungermann et al. (1999), who showed that V-ATPase activity is needed for *in vitro* homotypic fusion processes in yeast. This may relate to the recently published data on the participation of the Vma3p of V-ATPase's V_o sector in membrane fusion processes (Peters et al., 2001). Numerous protein complexes are involved in membrane fusion, a process that is not yet completely resolved (Wickner and Haas, 2000; Pelham, 2001). The fact that V-ATPase is suggested as taking part in various stages of this process, and that there are multiple spontaneous revertants of V-ATPase null mutants (Cohen et al., 1999), hint that the suppressor mutations come from the vast pool of the fusion machinery.

We thank Dr A. Bardul for his assistance with the confocal microscopy analysis, and Professor G. Schatz for the gift of FM4-64 and LysoSensor Green DND-189. This project has been funded by the BMBF and supported by BMBF's International Bureau at the DLR.

References

Clague, M. J., Urbe, S., Aniento, F. and Gruenberg, J. (1994). Vacuolar ATPase activity is required for endosomal carrier vesicle formation. *J. Biol. Chem.* **269**, 21–24.

Clague, M. J. (1998). Molecular aspects of the endocytic pathway. *Biochem. J.* **336**, 271–282.

Cohen, A., Perzov, N., Nelson, H. and Nelson, N. (1999). A novel family of yeast chaperons involved in the distribution of V-ATPase and other membrane proteins. *J. Biol. Chem.* **274**, 26885–26893.

Cousin, M. A. and Nicholls, D. G. (1997). Synaptic vesicle recycling in cultured cerebellar granule cells: role of vesicular acidification and refilling. *J. Neurochem.* **69**, 1927–1935.

D'Hondt, K., Heese-Peck, A. and Riezman, H. (2000). Protein and lipid requirements for endocytosis. *Annu. Rev. Genet.* **34**, 255–295.

Futai, M., Oka, T., Sun-Wada, G., Moriyama, Y., Kanazawa, H. and Wada, Y. (2000) Luminal acidification of diverse organelles by V-ATPase in animal cells. *J. Exp. Biol.* **203**, 107–116.

Grabe, M. and Oster, G. (2001). Regulation of organelle acidity. *J. Gen. Physiol.* **117**, 329–344.

Graham, T. R., Seeger, M., Payne, G. S., MacKay, V. L. and Emr, S. D. (1994). Clathrin-dependent localization of alpha 1,3 mannosyltransferase to the Golgi complex of *Saccharomyces cerevisiae*. *J. Cell Biol.* **127**, 667–678.

Graham, T. R. and Krasnov, V. A. (1995). Sorting of yeast alpha 1,3 mannosyltransferase is mediated by a lumenal domain interaction, and a transmembrane domain signal that can confer clathrin-dependent Golgi localization to a secreted protein. *Mol. Biol. Cell.* **6**, 809–824.

Grunow, A., Rusing, M., Becker, B. and Melkonian, M. (1999). V-ATPase is a major component of the Golgi complex in the scaly green flagellate *Scherffelia dubia*. *Protist* **150**, 265–281.

Guttenberger, M. (2000). Arbuscules of vesicular-arbuscular mycorrhizal fungi inhabit an acidic compartment within plant roots. *Planta* **211**, 299–304.

Kawasaki-Nishi, S., Nishi, T. and Forgac, M. (2001). Yeast V-ATPase complexes containing different isoforms of the 100-kDa a-subunit differ in coupling efficiency and *in vivo* dissociation. *J. Biol. Chem.* **276**, 17941–17948.

Llopis, J., McCaffery, J. M., Miyawaki, A., Farquhar, M. G. and Tsien, R. Y. (1998). Measurement of cytosolic, mitochondrial, and Golgi pH in single living cells with green fluorescent proteins. *Proc. Natl. Acad. Sci. USA* **95**, 6803–6808.

Lupashin, V. V., Pokrovskaya, I. D., McNew, J. and Waters, M. G. (1997). Characterization of a Novel Yeast SNARE Protein Implicated in Golgi Retrograde Traffic. *Mol. Biol. Cell* **8**, 2659–2676.

Lyons, S. and Nelson, N. (1984). An immunological method for detecting gene expression in yeast colonies. *Proc. Natl. Acad. Sci. USA* **81**, 7426–7430.

Manolson, M. F., Proteau, D., Preston, R. A., Stenbit, A., Roberts, T., Hoyt, M. A., Preuss, D., Mulholland, J., Botstein, D. and Jones, E. W. (1992). The *VPH1* gene encodes a 95-kDa integral membrane polypeptide required for *in vivo* assembly and activity of the yeast vacuolar H^+-ATPase. *J. Biol. Chem.* **267**, 14294–14303.

Manolson, M. F., Wu, B., Proteau, D., Taillon, B. E., Roberts, B. T., Hoyt, M. A. and Jones, E. W. (1994). *STV1* gene encodes functional homologue of 95-kDa yeast vacuolar H^+-ATPase subunit Vph1p. *J. Biol. Chem.* **269**, 14064–14074.

Mellman, I., Fuchs, R. and Helenius, A. (1986). Acidification of the endocytic and exocytic pathways. *Annu. Rev. Biochem.* **55**, 663–700.

Moriyama, Y. and Nelson, N. (1989). H^+-translocating ATPase in Golgi apparatus: Characterization as vacuolar H^+-ATPase and its subunit structures. *J. Biol. Chem.* **264**, 18445–18450.

Munn, A. L. and Riezman, H. (1994). Endocytosis is required for the growth of vacuolar H^+-ATPase-defective yeast: Identification of six new *END* genes. *J. Cell Biol.* **127**, 373–386.

Nelson, H. and Nelson, N. (1990). Disruption of genes encoding subunits of yeast vacuolar H^+-ATPase causes conditional lethality. *Proc. Natl. Acad. Sci. USA* **87**, 3503–3507.

Nelson, N. (1983). Structure and synthesis of chloroplast ATPase. *Methods Enzymol.* **97**, 510–523.

Nelson, N. and Harvey, W. R. (1999). Vacuolar and plasma membrane proton-adenosinetriphosphatases. *Physiol Rev.* **79**, 361–385.

Nothwehr, S. F., Conibear, E. and Stevens, T. H. (1995). Golgi and vacuolar membrane proteins reach the vacuole in vps1 mutant yeast cells via the plasma membrane. *J. Cell Biol.* **129**, 35–46.

Noumi, T., Beltrán, C., Nelson, H. and Nelson, N. (1991). Mutational analysis of yeast vacuolar H^+-ATPase. *Proc. Natl. Acad. Sci. USA* **88**, 1938–1942.

Pelham, H. R. (2001). SNAREs and the specificity of membrane fusion. *Trends Cell Biol.* **11**, 99–101

Perzov, N., Nelson, H. and Nelson, N. (2000). Altered distribution of the yeast plasma membrane H^+-ATPase as a feature of vacuolar H^+-ATPase null mutants. *J. Biol. Chem.* **275**, 40088–40095.

Peters, C., Bayer, M. J., Buhler, S., Andersen, J. S., Mann, M. and Mayer, A. (2001). Trans-complex formation by proteolipid channels in the terminal phase of membrane fusion. *Nature* **409**, 581–588.

Powell, B., Graham, L. A. and Stevens, T. H. (2000). Molecular characterization of the yeast vacuolar H^+-ATPase proton pore. *J. Biol. Chem.* **275**, 23654–23660.

Raymond, C. K., Howald-Stevenson, I., Vater, C. A. and Stevens, T. H. (1992). Morphological classification of the yeast vacuolar protein sorting mutants: evidence for a prevacuolar compartment in class E vps mutants. *Mol. Biol. Cell* **3**, 1389–1402.

Schapiro, F. B. and Grinstein, S. (2000). Determinants of the pH of the Golgi complex. *J. Biol. Chem.* **275**, 21025–21032.

Schoonderwoert, V. T., Holthuis, J. C., Tanaka, S., Tooze, S. A. and Martens, G. J. (2000). Inhibition of the vacuolar H^+-ATPase perturbs the transport, sorting, processing and release of regulated secretory proteins. *Eur. J. Biochem.* **267**, 5646–5654.

Stevens, T. H. and Forgac, M. (1997). Structure, function and regulation of the vacuolar (H^+)-ATPase. *Annu. Rev. Cell Dev. Biol.* **13**, 779–808.

Supek, F., Supekova, L. and Nelson, N. (1994). Features of vacuolar H^+-ATPase revealed by yeast suppressor mutants. *J. Biol. Chem.* **269**, 26479–26485.

Toyomura, T., Oka, T., Yamaguchi, C., Wada, Y. and Futai, M. (2000). Three subunit a isoforms of mouse vacuolar H(+)-ATPase. Preferential expression of the a3 isoform during osteoclast differentiation. *J. Biol. Chem.* **275**, 8760–8765.

Uchida, E., Ohsumi, Y. and Anraku, Y. (1985). Purification and properties of H^+-translocating, Mg^{2+}-adenosine triphosphatase from vacuolar membranes of *Saccharomyces cerevisiae*. *J. Biol. Chem.* **260**, 1090–1095.

Ungermann, C., Wickner, W. and Xu, Z. (1999). Vacuole acidification is required for trans-SNARE pairing, LMA1 release, and homotypic fusion. *Proc. Natl. Acad. Sci. USA* **96**, 11194–11199.

van Deurs, B., Holm, P. K. and Sandvig, K. (1996). Inhibition of the vacuolar H(+)-ATPase with bafilomycin reduces delivery of internalized molecules from mature multivesicular endosomes to lysosomes in HEp-2 cells. *Eur. J. Cell Biol.* **69**, 343–350.

van Weert, A. W., Dunn, K. W., Gueze, H. J., Maxfield, F. R. and Stoorvogel, W. (1995). Transport from late endosomes to lysosomes, but not sorting of integral membrane proteins in endosomes, depends on the vacuolar proton pump. *J. Cell Biol.* **130**, 821–834.

Vida, T. A. and Emr, S. D. (1995). A new vital stain for visualizing vacuolar membrane dynamics and endocytosis in yeast. *J. Cell Biol.* **128**, 779–792.

Wendland, B., Emr, S. D. and Riezman, H. (1998). Protein traffic in the yeast endocytic and vacuolar protein sorting pathways. *Curr. Opin. Cell. Biol.* **10**, 513–522.

Wickner, W. and Haas, A. (2000). Yeast homotypic vacuole fusion: a window on organelle trafficking mechanisms. *Annu. Rev. Biochem.* **69**, 247–275.

Ying, M., Flatmark, T. and Saraste, J. (2000). The p58-positive pre-Golgi intermediates consist of distinct subpopulations of particles that show differential binding of COPI and COPII coats and contain vacuolar H(+)-ATPase. *J. Cell Sci.* **113**, 3623–3638.

Yoshida, S. and Anraku, Y. (2000). Characterization of staurosporine-sensitive mutants of *Saccharomyces cerevisiae*: vacuolar functions affect staurosporine sensitivity. *Mol. Gen. Genet.* **263**, 877–888.